Scope and Mechanism of Alkene Hydrogenation/Isomerization Catalyzed by Complexes of the Type $R_2E(CH_2)_2M(CO)(L)$ (R = Cp, Me, Ph; E = P, Ta; M = Rh, Ir; L = CO, PPh_3)

Michael J. Hostetler, Matthew D. Butts, and Robert G. Bergman*

Contribution from the Department of Chemistry, University of California, Berkeley, California 94720

Received July 13, 1992

Abstract: The mechanism of the catalytic hydrogenation of alkenes by the early–late transition metal heterobimetallic (ELHB) complex $Cp_2Ta(CH_2)_2Ir(CO)_2$ (**1a**) has been studied. The first step is the oxidative addition of H_2, the product of which cannot be spectroscopically detected for **1a** but has been characterized by NMR spectroscopy for the related compound $Cp_2Ta(CH_2)_2Ir(CO)(PPh_3)$ (**2a**). The reaction of D_2 with **1a** and **2a** results in deuterium incorporation into the methylene bridges. We suggest that this reaction occurs by oxidative addition of D_2, reductive elimination of a μ-methylene deuteride to form a Ta–CH_2D group, C–H oxidative addition of this group across the iridium center, and reductive elimination of HD. We have studied the kinetics of this reaction and found that the rate is dependent upon [**1a**] and [D_2] and that the rate constant for this second-order reaction (k_{2nd}) at 35 °C is 2.57×10^{-2} M^{-1} s^{-1} is much larger than that for ethylene hydrogenation. In the hydrogenation, we further propose that the alkene binds to the species formed by reductive elimination of the μ-methylene hydride. Alkene then inserts into the Ir–H bond to form an iridium alkyl. This complex is a 4-coordinate iridium species and can thus readily β-eliminate, the result of which is that substituted alkenes are isomerized. Hydrogenation is completed by oxidative addition of the tantalum methyl C–H bond across the iridium center to form a 6-coordinate Ir(III) species, followed by reductive elimination of the alkyl hydride to form the free alkane. In the case of ethylene hydrogenation, the rate is dependent upon [**1a**], [H_2], and [C_2H_4], and the rate constant k_{3rd} for this third-order process at 45 °C is 9.21×10^{-2} M^{-2} s^{-1}. The rate of isomerization of 1-butene is approximately half that of hydrogenation; this process leads to a thermodynamic mixture of *cis*- and *trans*-2-butene. We have performed studies on the rate and scope (with ethylene, propene, 1-butene, and *cis*-2-butene) of hydrogenation/isomerization by seven other related catalyst systems: $Cp_2Ta(CH_2)_2Ir(CO)(PPh_3)$; the Ta–Rh analogues of the Ta–Ir catalysts, $Cp_2Ta(CH_2)_2Rh(CO)_2$ and $Cp_2Ta(CH_2)_2Rh(CO)(PPh_3)$; and the phosphorus ylide analogues of the Ta compounds bearing CO and PPh_3 ligands, $Ph_2P(CH_2)_2Ir(CO)(PPh_3)$, $Me_2P(CH_2)_2Ir(CO)(PPh_3)$, $Ph_2P(CH_2)_2Rh(CO)(PPh_3)$, and $Me_2P(CH_2)_2Rh(CO)(PPh_3)$. The tantalum–iridium species hydrogenate alkenes up to 150 times faster than the ylide complexes, but the Ta–Rh compounds hydrogenate alkenes at about the same rate as their P–Rh analogues. Both Ta–Ir species undergo exchange of deuterium into the μ-CH_2 groups faster than hydrogenation, both Ta–Rh complexes undergo exchange more slowly than hydrogenation, and none of the four ylide compounds exchange. Only $Cp_2Ta(CH_2)_2Rh(CO)(PPh_3)$ isomerizes 1-butene in the absence of hydrogen. Addition of mercury normally has no effect on these hydrogenations, indicating that they are homogeneous processes. The sole exception is in reactions of $Cp_2Ta(CH_2)_2Rh(CO)_2$ where hydrogenation is spoiled upon addition of mercury to the system, indicating that a colloid may be the active species in this case. Hydrogenation by all of the ylide complexes is inhibited by PPh_3, and thus in these cases the mechanism is proposed to involve PPh_3 dissociation.

Introduction

The strong metal support interaction (SMSI) is a phenomenon in which the catalytic properties of a later transition metal film are significantly altered by the presence of an early transition metal support.[1,2] Because the possibility exists that an early–late heterobimetallic (ELHB) complex could also exhibit such effects, much work has been directed toward the synthesis of this class of compounds.[3-9] However, despite the large number of ELHB complexes reported, only a few studies on their catalytic behavior are available.[10-12] Thus, when we discovered a series of catalytically active ELHB complexes,[13] we initiated a systematic mechanistic study that would help to define the role of these species as catalytic agents.

The hydrogenation of alkenes by mononuclear transition metal catalysts is a well-studied process with several landmark publications covering a wide variety of mechanisms.[14,15] For late transition metal systems, there are three commonly proposed mechanisms (Scheme I): (1) Monohydride catalysts, such as $HRh(CO)(PPh_3)_3$, operate via sequential ligand loss, binding of an alkene, insertion of the alkene into the M–H bond, oxidative addition of hydrogen, and then reductive elimination of the alkane

(1) *Metal-Support Interactions in Catalysis, Sintering, and Redispersion*; Stevenson, S. A., Dumesic, J. A., Baker, R. T. K., Ruckenstein, E., Eds.; Van Nostrand: New York, 1987.
(2) Imelik, B.; Naccache, C.; Coudurier, G.; Praliaud, J.; Meriaudeau, P.; Gallezot, P.; Martin, G. A.; Vedrine, J. C. *Metal-Support and Metal-Additive Effects in Catalysis*; Elsevier: New York, 1982.
(3) For a review, see: Stephan, D. W. *Coord. Chem. Rev.* **1989**, *95*, 41.
(4) Jacobsen, E. N.; Goldberg, K. I.; Bergman, R. G. *J. Am. Chem. Soc.* **1988**, *110*, 3706.
(5) Goldberg, K. I.; Bergman, R. G. *J. Am. Chem. Soc.* **1988**, *110*, 4853.
(6) Vites, J. C.; Steffey, B. D.; Giuseppetti-Dery, M. E.; Cutler, A. R. *Organometallics* **1991**, *10*, 2827.
(7) Katti, K. V.; Cavell, R. G. *Organometallics* **1991**, *10*, 539.
(8) Selent, D.; Beckhaus, R.; Bartik, T. *J. Organomet. Chem.* **1991**, *405*, C15.
(9) McFarland, J. M.; Churchill, M. R.; See, R. F.; Lake, C. H.; Atwood, J. D. *Organometallics* **1991**, *10*, 3530.
(10) Baker, R. T.; Glassman, T. E.; Ovenall, D. W.; Calabrese, J. C. *Isr. J. Chem.* **1991**, *31*, 33.
(11) Gelmini, L.; Stephan, D. W. *Organometallics* **1988**, *7*, 849.
(12) Choukroun, R.; Gervais, D.; Jaud, J.; Kalck, P.; Senocq, R. *Organometallics* **1986**, *5*, 67.
(13) Hostetler, M. J.; Bergman, R. G. *J. Am. Chem. Soc.* **1990**, *112*, 8621.
(14) Collman, J. P.; Hegedus, L. S.; Norton, J. R.; Finke, R. G. *Principles and Applications of Organotransition Metal Chemistry*; University Science Books: Mill Valley, CA, 1987; Chapter 10.
(15) James, B. R. In *Comprehensive Organometallic Chemistry*; Wilkinson, G., Stone, F. G. A., Abel, E. W., Eds.; Pergamon: New York, 1982; Vol. 8, Chapter 51.

0002-7863/93/1515-2743$04.00/0

Scheme I

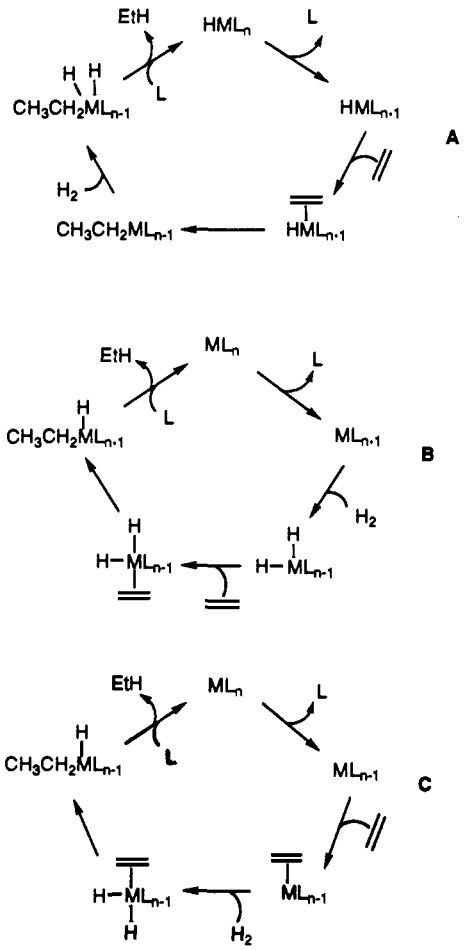

(mechanism A).[14] (2) Catalysts that form dihydrides, such as $(PPh_3)_3RhCl$, often follow a pathway consisting of ligand loss, oxidative addition of hydrogen, binding of an alkene, insertion of the alkene into the M–H bond, and then reductive elimination of the alkane (mechanism B).[16,17] (3) Catalysts such as $[RhL_2(S)_2]^+$ hydrogenate alkenes via a route consisting of ligand loss, binding of an alkene, oxidative addition of hydrogen, insertion of the alkene into the M–H bond, and then reductive elimination of the alkane (mechanism C).[18-20]

Herein, we present our detailed study of the scope and mechanism of alkene hydrogenation and isomerization by the ELHB complexes $Cp_2Ta(CH_2)_2Ir(CO)(L)$ [L = CO (**1a**), PPh_3 (**2a**)]. In addition, we report the catalytic activity of the rhodium analogues of **1a** and **2a**, $Cp_2Ta(CH_2)_2Rh(CO)(L)$ [L = CO (**1b**), PPh_3 (**2b**)]. Finally, to identify the effect that the early metal fragment has on the hydrogenation occurring at the late metal, we present the synthesis, characterization, and catalytic reactivity of the model compounds $R_2P(CH_2)_2M(CO)(PPh_3)$ [R = Ph, M = Ir (**4a**), Rh (**4b**); R = Me, M = Ir (**5a**), Rh (**5b**)], in which the Cp_2Ta fragment has been replaced with either a Ph_2P or a Me_2P fragment. This allows us to take the molecular chassis, $E(CH_2)_2M(CO)(L)$, and study how a change in each of its components (i.e., E = Cp_2Ta, R_2P; R = Me, Ph; M = Rh, Ir; L = CO, PPh_3) affects not only its ability to catalyze the hydrogenation of alkenes but also the mechanism by which it operates.

Results

Synthesis of the Catalysts. Compound **1a** was synthesized by the reaction of $Cp_2Ta(CH_2)(CH_3)$ with indenyliridium dicarbonyl

Scheme II

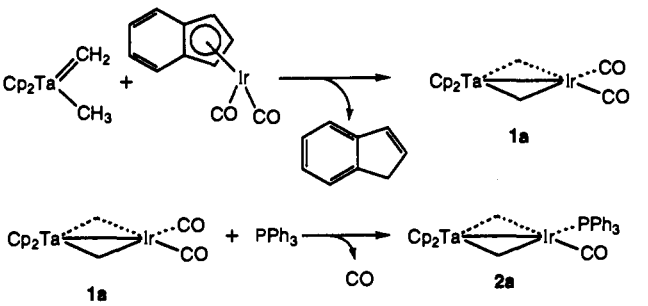

Scheme III

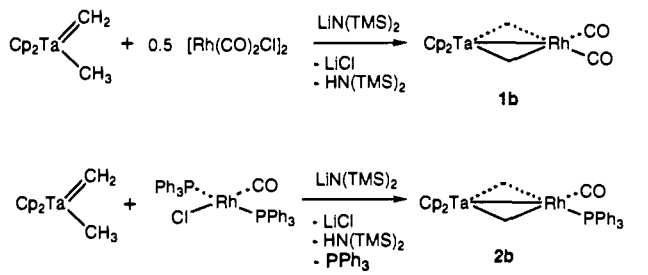

Scheme IV

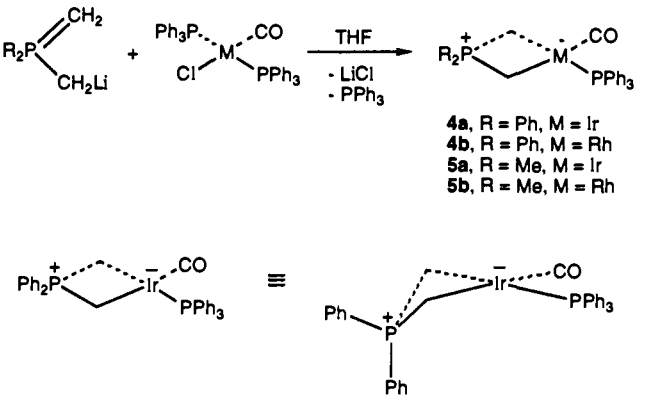

(IndIr(CO)$_2$).[21] The reaction of **1a** with PPh_3 then leads to the formation of the substitution product $Cp_2Ta(CH_2)_2Ir(CO)(PPh_3)$ (**2a**), in which the iridium center is 4-coordinate (Scheme II). Consistent with this formulation, only a single CO stretch at 1934 cm^{-1} is present in the IR spectrum. The Cp groups are equivalent and the CH_2 groups inequivalent, as shown by both ^1H and $^{13}C\{^1H\}$ NMR spectroscopy. The $^{31}P\{^1H\}$ NMR spectrum and the elemental analysis of **2a** are also consistent with the replacement of a CO ligand by PPh_3.

The Ta–Rh complexes, $Cp_2Ta(CH_2)_2Rh(CO)_2$ (**1b**) and $Cp_2Ta(CH_2)_2Rh(CO)(PPh_3)$ (**2b**), were prepared by the base $(LiN(TMS)_2)$ promoted reaction of $Cp_2Ta(CH_2)(CH_3)$ with $[Rh(CO)_2Cl]_2$ and $ClRh(CO)(PPh_3)_2$, respectively (Scheme III).[22] The spectroscopic properties of **1b** and **2b** are nearly identical to those of their iridium analogues.

Reaction of the deprotonated ylide $Ph_2P(CH_2)_2Li$[23-25] with the compounds $ClIr(CO)(PPh_3)_2$ and $ClRh(CO)(PPh_3)_2$ results in the formation of $Ph_2P(CH_2)_2M(CO)(PPh_3)$ (**4a** and **4b**, respectively), with the loss of 1 equiv of PPh_3 (Scheme IV). Similarly, the reaction of $Me_2P(CH_2)_2Li$ with $ClIr(CO)(PPh_3)_2$ and $ClRh(CO)(PPh_3)_2$ leads to the synthesis of $Me_2P(CH_2)_2$-$M(CO)(PPh_3)$ (**5a** and **5b**, respectively) (Scheme IV).[26] Each

(16) Dawans, F.; Morel, D. *J. Mol. Catal.* **1977–8**, *3*, 403.
(17) Halpern, J. *J. Mol. Catal.* **1976**, *2*, 65.
(18) Chan, A. S. C.; Halpern, J. *J. Am. Chem. Soc.* **1980**, *102*, 838.
(19) Halpern, J. *Science (Washington, D.C.)* **1982**, *217*, 401.
(20) Halpern, J.; Riley, D. P.; Chan, A. S. C.; Pluth, J. J. *J. Am. Chem. Soc.* **1977**, *99*, 8055.
(21) Hostetler, M. J.; Butts, M. D.; Bergman, R. G. *Inorg. Chim. Acta* **1992**, *198–200*, 377.
(22) Butts, M. D.; Hostetler, M. J.; Bergman, R. G. Manuscript in preparation.
(23) Manzer, L. E. *Inorg. Chem.* **1976**, *15*, 2567.
(24) Fandos, R.; Gomez, M.; Royo, P. *Organometallics* **1989**, *8*, 1604.
(25) Cramer, R. E.; Roth, S.; Edelmann, F.; Bruck, M. A.; Cohn, K. C.; Gilje, J. W. *Organometallics* **1989**, *8*, 1192.

Scheme V

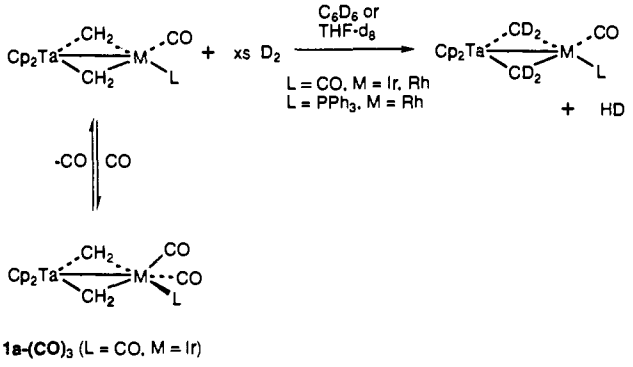

1a-(CO)$_3$ (L = CO, M = Ir)

Scheme VI

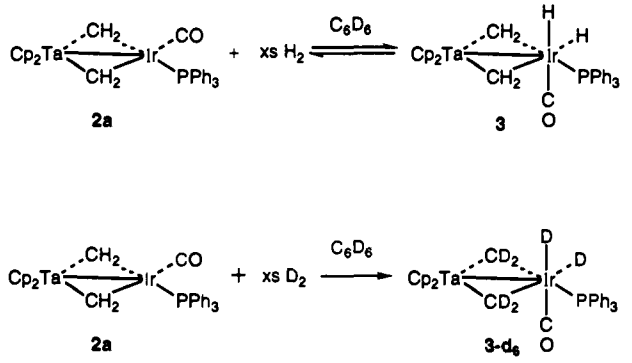

of these compounds, **4a,b**, **5a,b**, exhibits temperature-dependent behavior in solution as determined by variable-temperature NMR studies, and the spectroscopic properties of **4a** and **5a** have been described.[21] The spectroscopic properties of the Rh complexes **4b** and **5b** were found to be quite similar to those of the iridium ylide compounds, and the same interpretation has been applied. On the basis of the variable-temperature NMR studies, the fluxionality is believed to involve rapid ring inversion in the puckered four-membered ring and reversible loss of the phosphine ligand. An X-ray crystallographic study was performed on **4a**, confirming the structure shown in Scheme IV.[21]

Reactions with H_2 and D_2. Compound **1a** does not react with H_2 to give an isolable or observable iridium(III) species. However, like $Cp_2Ta(CH_2)_2Pt(H)(PMe_3)$,[4] reaction of **1a** with excess D_2 results in the disappearance of the μ-CH_2 resonance in the ^1H NMR spectrum with the simultaneous appearance of the HD resonance (Scheme V). The ^2H NMR spectrum of isolated **1a**-d_4 revealed that only the μ-CH_2 groups had been deuterated; mass spectroscopy confirmed the incorporation of four deuterons.

In contrast to **1a**, compound **2a** reacted with H_2 to give the spectroscopically characterized oxidative addition product $Cp_2Ta(CH_2)_2Ir(H)_2(CO)(PPh_3)$ (**3**); upon removal of the hydrogen atmosphere, **3** reverts to **2a** (Scheme VI). There are two hydride signals with similar H–P coupling constants in the ^1H NMR spectrum of **3**. The $^{13}C\{^1H\}$ NMR spectrum reveals two different CH_2 groups, one with a J_{CP} of 35.6 Hz and the other with a J_{CP} of 2.3 Hz, indicating the PPh_3 is trans to one CH_2 and cis to the other. Thus, the hydrogen adds over the Ir–CO bond,[27,28] leaving both Ir–H groups cis to PPh_3. No sign of the other isomer, in which the H_2 adds over the Ir–PPh_3 bond, is ever observed. Reaction of **2a** with excess D_2 results in the production of both **2a** and **3** with fully deuterated CH_2 groups.

The equilibrium constant for the reaction of H_2 with $Cp_2Ta(CH_2)_2Ir(CO)(PPh_3)$ in toluene-d_8 was measured by ^1H NMR spectroscopy over the temperature range 22–80 °C. From these data, the thermodynamic parameters for the reaction were calculated: $\Delta H° = -12.0 \pm 0.2$ kcal/mol and $\Delta S° = -23.7 \pm 0.6$ eu.[29]

Scheme VII

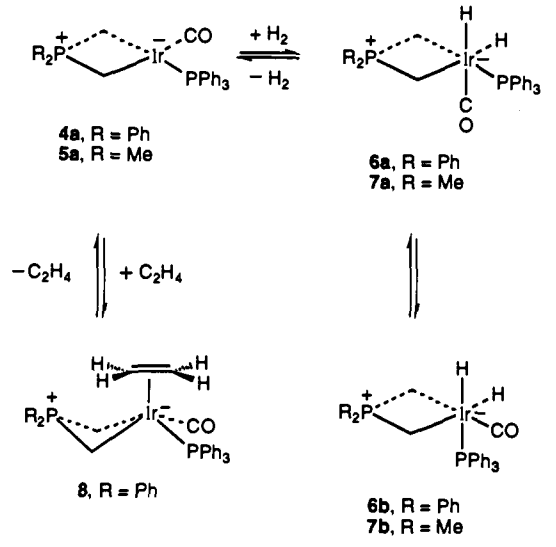

Addition of H_2 to a solution of either Ta–Rh compound did not produce an observable oxidative addition product. However, as in the case of the Ta–Ir compounds, addition of excess D_2 resulted in the complete incorporation of deuterium into the bridging methylene positions (Scheme V). Both Ta–Rh complexes slowly decompose under an H_2 atmosphere to form uncharacterized products.

The ylide P–Ir complexes also react with H_2 to form spectroscopically characterized oxidative addition products. For example, compound **4a** reacts reversibly with H_2 to form **6a,b** (Scheme VII); upon removal of the hydrogen atmosphere, both species revert to **4a**. Isomer **6a**, with hydride resonances at δ –7.7 and –12.8 (J_{PH} = 20.4 and 13.6 Hz, respectively), forms initially. After 4 h at room temperature, isomer **6b**, with hydride resonances at δ –8.1 and –11.6 (J_{PH} = 44.9 and 14.2 Hz, respectively), can be detected in the ^1H NMR spectrum. The structures of **6a,b** were assigned on the basis of their P–H and P–C coupling constants. Compound **5a** exhibits similar behavior under a hydrogen atmosphere, with the immediate formation of **7a** under H_2 followed by the slow conversion to **7b**. The ylide P–Rh compounds **4b** and **5b**, like their Ta–Rh analogues, do not show any oxidative addition products with hydrogen. In contrast, however, to the reactivity observed for the heterobimetallic complexes, the addition of D_2 to phosphine complexes **4a**, **4b**, **5a**, or **5b** does not result in the incorporation of deuterium into the bridging methylene sites even after several days at 45 °C.

Determination of the Rate Law for Deuterium Exchange. The rate of deuterium exchange into the CH_2 groups of **1a** was measured under a variety of conditions (Table I and Figure 1). As can be seen, the rate is linearly dependent upon the concentrations of both D_2 and **1a** (i.e., $d[\mathbf{1a}]/dt = k_{2nd}[\mathbf{1a}][D_2]$). The value for the second-order rate constant k_{2nd} is 2.57×10^{-2} M^{-1} s^{-1} at 35 °C in toluene-d_8. No solvent effect was observed for solutions of **1a** in THF-d_8 and C_6D_6 under identical amounts of D_2. Added CO inhibits the reaction[30] by forming what is assigned to be the 18 e$^-$ tricarbonyl compound **1a**-$(CO)_3$ (Scheme V).[31] After addition of 1350 Torr of CO, the CH_2 and Cp resonances in the ^1H NMR spectrum became broad, even though

(26) For reviews on transition metal ylide complexes, see: (a) Schmidbauer, H. *Angew. Chem., Int. Ed. Engl.* **1983**, *22*, 907. (b) Kaska, W. C. *Coord. Chem. Rev.* **1983**, *48*, 1. (c) Schmidbauer, H. *Acc. Chem. Res.* **1975**, *8*, 62.

(27) Deutsch, P. P.; Eisenberg, R. *Chem. Rev.* **1988**, *88*, 1147.

(28) Sargent, A. L.; Hall, M. B.; Guest, M. F. *J. Am. Chem. Soc.* **1992**, *114*, 517.

(29) Hostetler, M. J.; Bergman, R. G. *J. Am. Chem. Soc.* **1992**, *114*, 7629.

(30) Hostetler, M. J. Ph.D. Thesis, University of California, Berkeley, 1992.

(31) For other iridium tricarbonyl complexes, see: (a) Whyman, R. *J. Organomet. Chem.* **1975**, *94*, 303. (b) Intelle, G. M.; Graithwhite, M. J. *J. Chem. Soc., Dalton Trans.* **1972**, 645. (c) Collman, J. P.; Vastine, F. D.; Roper, W. R. *J. Am. Chem. Soc.* **1968**, *90*, 2282.

Table I. Rate Data for the Incorporation of Deuterium into the CH_2 Groups of **1a** in Toluene-d_8[a]

T (°C)	k_{obs} (s^{-1})	$[D_2]$[b] (M)	k_{2nd}[c] (M^{-1} s^{-1})
20	1.92×10^{-5}	2.63×10^{-3}	7.30×10^{-3}
20	3.81×10^{-5}	5.27×10^{-3}	7.23×10^{-3}
20	4.94×10^{-5}	7.78×10^{-3}	6.35×10^{-3}
20	5.62×10^{-5}	9.63×10^{-3}	5.84×10^{-3}
0	1.57×10^{-5}	7.52×10^{-3}	2.09×10^{-3}
35	2.60×10^{-4}	1.01×10^{-2}	2.57×10^{-2}
50	4.05×10^{-4}	1.06×10^{-2}	3.82×10^{-2}

[a] See the Experimental Section for details of the setup procedure. [b] Concentration of D_2 was based upon a $[H_2]$ vs T plot under similar conditions. The increased concentration of gas present at elevated temperatures is the result of greater gas pressure added to the NMR tube. [c] The error limits for k_{2nd} were estimated to be ±10% on the basis of the reproducibility of the values and the uncertainty in $[D_2]$.

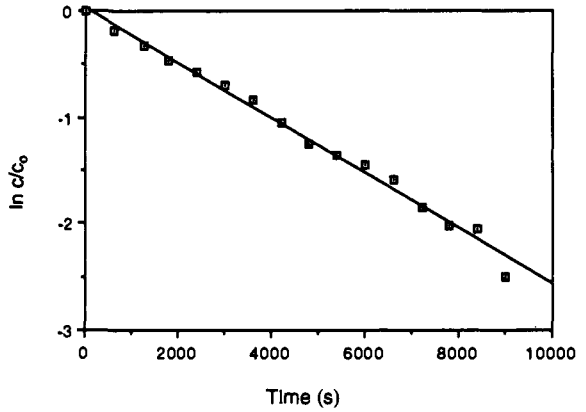

Figure 1. Plot of ln c/c_0 vs time for the incorporation of deuterium into **1a** at 35 °C in toluene-d_8. The disappearance of the μ-CH_2 group in the ^1H NMR spectrum was monitored ($k_{obs} = 2.60 \times 10^{-4}$ s^{-1}; $r^2 = 0.991$).

the chemical shifts changed only slightly. Identical solution behavior was seen for the compound $Cp_2Ta(CH_2)_2Ir(PEt_3)(CO)_2$.[21]

Reactions with Ethylene. Upon addition of ethylene, an equilibrium is established between compound **4a** and an addition complex (Scheme VII). The equilibrium lies toward uncoordinated ethylene (15 equiv) and **4a** at room temperature. The addition complex can be detected at low temperature by $^{13}C\{^1H\}$ NMR spectroscopy and is thought to have structure **8**. The carbon spectrum contains two singlets attributed to bound ethylene at 23.8 and 13.0 ppm. The CO appears as a doublet ($J_{CP} = 8.2$ Hz), consistent with coupling to a cis phosphorus atom. One of the bridging methylene carbons appears as a doublet and the other as a doublet of doublets, supporting the proposed square-based pyramid structure. In the ^1H NMR spectrum, the alkyl region of **8** could not be resolved even at −80 °C. No reaction was observed between ethylene and the other binuclear compounds.

Catalytic Hydrogenation and Isomerization: Determination of the Rate Laws for Hydrogenation. Compound **1a** catalytically hydrogenates ethylene at 45 °C under H_2 to form ethane. The catalyst appears to be robust. For example, a hydrogenation in one reaction vessel was allowed to proceed for 40 turnovers. When the atmosphere above the solution was removed and the vessel repressurized with H_2 and C_2H_4, the catalyst was just as active as before.

Because two of the reagents are gases and hydrogen does not condense (at 77 K), the rate law was determined by first ensuring a linear dependence on [**1a**] (i.e., when [**1a**] was doubled, the rate of hydrogenation doubled). Then, the dependence on $[C_2H_4]$ and $[H_2]$ was determined by measuring the effect of varying their concentrations on the initial turnover rate (10 ± 5% reaction) (Table II). As can be seen, the initial rate of alkene hydrogenation is dependent upon the concentrations of H_2 (Figure 2) and ethylene (Figure 3) (i.e., rate = k[**1a**]$[C_2H_4][H_2]$). It was possible to measure the absolute rather than the initial rate constant at low

Table II. Turnover Data Used for the Derivation of the Rate Law for Ethylene Hydrogenation by **1a**[a]

$[C_2H_4]$[b] (M)	$[H_2]$[c] (M)	turnovers/s[d]
1.07×10^{-2}	1.20×10^{-2}	1.05×10^{-5}
4.64×10^{-2}	1.39×10^{-2}	3.66×10^{-5}
1.21×10^{-1}	1.34×10^{-2}	1.31×10^{-4}
2.32×10^{-1}	1.36×10^{-2}	1.75×10^{-4}
3.91×10^{-1}	1.30×10^{-2}	2.62×10^{-4}
2.26×10^{-1}	4.01×10^{-3}	4.08×10^{-5}
2.18×10^{-1}	9.58×10^{-4}	1.36×10^{-5}
2.23×10^{-1}	2.92×10^{-4}	3.62×10^{-6}

[a] [**1a**] = 8.37×10^{-3} M; solvent = C_6D_6; T = 45 °C. [b] Determined by integrating against an internal standard in the ^1H NMR spectrum. [c] Calculated as 2.8% of the total amount of hydrogen added to the NMR tube (on the basis of previous experiments in which hydrogen concentration was measured by integrating against an internal standard in the ^1H NMR spectrum). [d] Calculated after 10 ± 5% of the reaction was complete. The error in the turnover number is estimated to be ±10%.

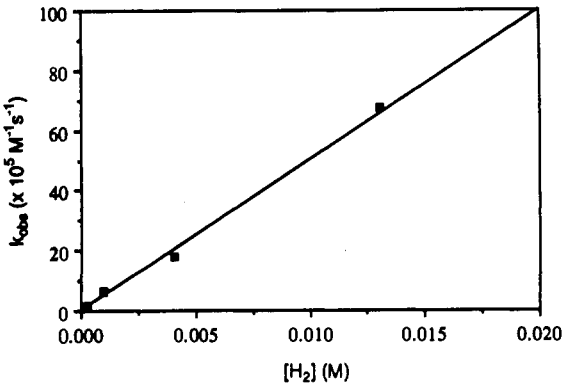

Figure 2. Plot of the observed rate constant (turnover number normalized to $[C_2H_4]$ = 1 M) vs $[H_2]$ ($r^2 = 0.997$) for the catalytic hydrogenation of ethylene by **1a** in C_6D_6 at 45 °C.

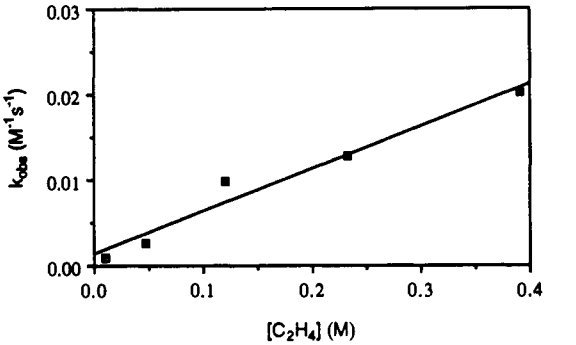

Figure 3. Plot of the observed rate constant (turnover number normalized to $[H_2]$ = 1 M) vs $[C_2H_4]$ ($r^2 = 0.966$) for the catalytic hydrogenation of ethylene by **1a** in C_6D_6 at 45 °C. Although the data must contain the origin as a point, to force the line to go through zero would overemphasize the error in the best fit line.

concentrations of ethylene and the highest possible concentration of H_2. The third-order rate constant for ethylene hydrogenation in toluene-d_8 at 45 °C is 9.21×10^{-2} M^{-2} s^{-1} (Figure 4). The isomerization of 1-butene by **1a** was found to follow a similar rate law.

The rate laws for hydrogenation catalyzed by the ylide complexes **4a,b** in the presence of added phosphine were also studied using the same method at 45 °C. From these studies, it was determined that the following reactions were first order in catalyst, alkene, and H_2: (1) ethylene hydrogenation by **4a** in C_6D_6; (2) propene hydrogenation by **4b** in C_6D_6. These reactions were found to be inhibited by the presence of added phosphine. The addition of 10 equiv of PPh_3 to an NMR tube containing an ylide catalyst, H_2, and ethylene slowed the rate of hydrogenation considerably (in turnover number; first 10 ± 5% of reaction). For compounds **4a** and **5a**, only trace amounts of ethane could be detected in the ^1H NMR spectrum after 3 days at 45 °C. When

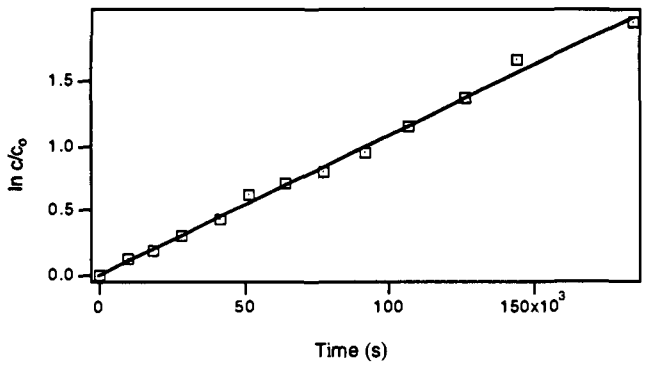

Figure 4. Plot of ln c/c_0 vs time for the hydrogenation of ethylene by **1a** in C_6D_6 at 45 °C with $[H_2] = 1.39 \times 10^{-2}$ M and [**1a**] $= 8.37 \times 10^{-3}$ M. The production of ethane was monitored over 2.75 half-lives ($k_{3rd} = 9.21 \times 10^{-2}$ M^{-2} s^{-1}).

Table III. Turnover Rates for the Hydrogenation of Alkenes by $Cp_2Ta(CH_2)_2Ir(CO)_2$ (**1a**) and $Cp_2Ta(CH_2)_2Ir(CO)(PPh_3)$ (**2a**)[a]

alkene (catalyst)	products[b]	time of one hydrogenation turnover (T, °C)
ethylene (**1a**)	ethane	1 h (45)
propene (**1a**)	propane	8 h (45)
1-butene (**1a**)	B:C:T = 1:1.2:1.3	6 h (45)
cis-2-butene (**1a**)	B:T = 0:1	2 days (45)[c]
ethylene (**2a**)	ethane	30 min (45)
1-butene (**2a**)	B:C:T = 3:1:1	75 min (45)
cis-2-butene (**2a**)	B:T = 1:2	90 min (66)
trans-2-butene (**2a**)	B:C = 3:4	2 h (66)
butadiene (**2a**)	B:O:C:T = 1:2:1:1	30 min (66)
cyclohexene (**2a**)	cyclohexane	2.5 h (66)

[a] See the Experimental Section for details; calculated after 10 ± 5% of the total reaction. [b] Product ratios are given where there are multiple products; B = butane; C = *cis*-2-butene; T = *trans*-2-butene; O = 1-butene. Ratios reported are those during the initial stage of the reaction (10 ± 5% of total reaction). [c] Time for one isomerization turnover.

25 equiv of PPh_3 was added to the rhodium ylide catalysts, H_2, and propene, a 7-fold decrease in rate was observed for **4b** and a 75-fold decrease for **5b**.

Catalytic Hydrogenation and Isomerization: Turnover Measurements. The relative activity of all of the catalysts reported here was measured by calculating the turnover rate within the first 10 ± 5% of the reaction (in this regime, c/c_0 is approximately equal to ln c/c_0). The hydrogenation reactions were run in the presence of approximately 5% catalyst with respect to alkene concentration with the exception of reactions catalyzed by **4a** (these reactions contained 15% catalyst due to the low activity of **4a**).

For compound **1a**, propene and 1-butene were hydrogenated about 7 times more slowly than ethylene in benzene at 45 °C (Table III). Under these conditions, 1-butene isomerized to an approximately thermodynamic mixture of *cis*- and *trans*-2-butene at a rate about half that of hydrogenation. Under an atmosphere of D_2, deuterium was incorporated into propane and "unreacted" propene (all positions appear to be approximately equally deuterated). The disubstituted alkene *cis*-2-butene was not hydrogenated and only slowly isomerized to *trans*-2-butene (one turnover in 2 days); isomerization to 1-butene was not observed. In order to test whether the active catalyst was formed by splitting of **1a** into two mononuclear fragments under hydrogenation conditions, ethylene hydrogenation was performed in the presence of $Cp_2Ta(CD_2)(CD_3)$. However, no sign of either $Cp_2Ta(CH_2)(CH_3)$ or **1a**-d_x was observed, indicating that fragmentation does not occur.

Substitution of triphenylphosphine for CO produced an improved catalyst (**2a**; Table III). Despite the increased steric bulk of PPh_3 relative to CO, the resulting compound hydrogenated substituted alkenes at rates significantly above those of the parent compound. While the rate for ethylene hydrogenation increased 2-fold relative that for **1a** (one turnover every 30 min at 45 °C), the rate for primary alkene hydrogenation, such as 1-butene, increased by nearly a factor of 5 (one turnover every 75 min at 45 °C); 1-butene was isomerized at a rate similar to that of hydrogenation. Disubstituted alkenes, such as *cis*-2-butene (one turnover every 90 min at 66 °C) and *trans*-2-butene (one turnover every 2 h at 66 °C), were hydrogenated and isomerized more slowly. Butadiene was hydrogenated at 45 °C (at about the same rate as 1-butene) to a 50:50 mixture of the 2-butenes and some 1-butene. Cyclohexene was hydrogenated to cyclohexane more slowly than any of the other alkenes tested (one turnover every 2.5 h at 66 °C). Thus **2a** appears to behave like a typical hydrogenation catalyst which is sensitive to the steric bulk of the alkene.[32,33]

Table IV. Turnover Rates for the Hydrogenation of Alkenes by $Cp_2Ta(CH_2)_2Rh(CO)_2$ (**1b**) and $Cp_2Ta(CH_2)_2Rh(CO)(PPh_3)$ (**2b**)[a]

alkene (catalyst)	products[b]	time for one hydrogenation turnover (T, °C)
ethylene (**1b**)	ethane	2.5 min (45)
propene (**1b**)	propane	17 min (45)
1-butene (**1b**)	B:C:T = 1:8:11	2 h (45)
cis-2-butene (**1b**)	B:T = 1:3	1.5 h (45)
ethylene (**2b**)	ethane	1 min (25)
propene (**2b**)	propane	9 min (45)
1-butene (**2b**)	B:C:T = 3:1:1	9 min (45)
cis-2-butene (**2b**)	B:T = 1:2	20 min (45)

[a] See the Experimental Section for details; calculated after 10 ± 5% of the total reaction. [b] Product ratios are given where there are multiple products; B = butane; C = *cis*-2-butene; T = *trans*-2-butene. Ratios reported are those during the initial stage of the reaction (10 ± 5% of total reaction).

Compounds **1b** and **2b**, the rhodium analogues of **1a** and **2a**, were much more active as alkene hydrogenation catalysts (Table IV). For example, the rate of ethylene hydrogenation by $Cp_2Ta(CH_2)_2Rh(CO)(PPh_3)$ (**2b**) was greater than the rate of hydrogen diffusion into the solution. This rate enhancement was less pronounced when substituted alkenes were used; for example, 1-butene was hydrogenated approximately 8 times faster with **2b** than with **2a**. Incorporation of D_2 into the bridging methylene positions occurs at approximately the same rate as that observed with **1a** or **2a**, but deuterium exchange into **2b** proceeds more slowly than the rate of alkene hydrogenation.

Addition of either CO or PPh_3 to any of the Ta–M complexes resulted in either decomposition or the formation of new species, and thus inhibition studies could not be performed. For example, addition of CO to **1a** resulted, as mentioned above, in the formation of **1a**-$(CO)_3$; addition of PPh_3 produced **2a**. Compound **2b** decomposes to uncharacterized products in the presence of excess PPh_3 under hydrogenation conditions. The addition of CO to **2b** did not lead to the 5-coordinate Rh species. The ^1H NMR spectrum of **2b** in C_6D_6 under an excess of CO consists of singlets at 5.56 and 4.46 ppm, which correspond to **1b**. The ^1H and $^{31}P\{^1H\}$ NMR spectra also contain broadened resonances for free PPh_3. These spectroscopic data are in agreement with ligand substitution to form the dicarbonyl compound, which continues to undergo ligand exchange with the liberated PPh_3.

Compound **1b** was the only catalyst studied in which hydrogenation was spoiled by the presence of mercury. Addition of 10 μL of Hg to an NMR tube containing **1b**, H_2, and C_2H_4 resulted in complete shutdown of the catalytic process. No metal-containing species other than **1b** could be detected. When propene, H_2, and CO were added together with **1b** and an excess of PPh_3, the hydrogenation catalyst $HRh(CO)(PPh_3)_3$ could be isolated in 25% yield. No tantalum-containing species could be isolated. An active catalyst is also formed when PPh_3 is not added to the

(32) Birch, A. J.; Williamson, D. H. *Org. React. (N.Y.)* **1976**, *24*, 1.
(33) James, B. R. *Homogeneous Hydrogenation*; Wiley: New York, 1973; Chapter XI.

Table V. Turnover Rates for the Hydrogenation of Alkenes by the Ylide Complexes $Ph_2P(CH_2)_2Ir(CO)(PPh_3)$ (**4a**), $Ph_2P(CH_2)_2Rh(CO)(PPh_3)$ (**4b**), $Me_2P(CH_2)_2Ir(CO)(PPh_3)$ (**5a**), and $Me_2P(CH_2)_2Rh(CO)(PPh_3)$ (**5b**)[a]

alkene (catalyst)	products[b]	time of one hydrogenation turnover (T, °C)
ethylene (**4a**)	ethane	24 h (45)
propene (**4q**)	propane	36 h (45)
1-butene (**4a**)	B:C:T = 0:1:1	8.5 h (45)[c]
cis-2-butene (**4a**)	B:T = 0:1	36 h (45)[c]
ethylene (**4b**)	ethane	4 min (25)
propene (**4b**)	propane	10 min (45)
1-butene (**4b**)	B:C:T = 1:1:1	11 min (45)
cis-2-butene (**4b**)	B:T = 1:3.5	50 min (45)
ethylene (**5a**)	ethane	1 h (45)
propene (**5a**)	propane	10.5 h (45)
1-butene (**5a**)	B:C:T = 4:1:1	13 h (45)
cis-2-butene (**5a**)	B:T = 1:3	14 h (45)
ethylene (**5b**)	ethane	2 min (25)
propene (**5b**)	propane	3 min (45)
1-butene (**5b**)	B:C:T = 1.3:1:1	5 min (45)
cis-2-butene (**5b**)	B:T = 1:2.5	7 min (45)

[a] See the Experimental Section for details; calculated after 10 ± 5% of the total reaction (note that the [**4a**] is approximately 3 times higher than that used for the other catalysts). [b] Product ratios are given where there are multiple products; B = butane; C = *cis*-2-butene; T = *trans*-2-butene. Ratios reported are those during the initial stage of the reaction (10 ± 5% of total reaction). [c] Time for one isomerization turnover.

reaction. This leads to a red oil which could not be purified or characterized.

The iridium ylide compound $Ph_2P(CH_2)_2Ir(CO)(PPh_3)$ (**4a**) catalyzed the hydrogenation and isomerization of alkenes at much slower rates (up to 150 times slower) than its bimetallic analogue **2a** (Table V). The hydrogenation of ethylene by **4a** at 45 °C proceeded at a rate of one turnover in 1 day and that of propene at one turnover in 1.5 days. 1-Butene and *cis*-2-butene were only isomerized, with one turnover occurring every 8.5 and 36 h, respectively. The more electron-rich $Me_2P(CH_2)_2Ir(CO)(PPh_3)$ (**5a**) was a better catalyst, hydrogenating even disubstituted alkenes.

The rhodium ylide compounds were better catalysts than their iridium counterparts (Table V). As with the Ta–Rh complexes, ethylene hydrogenation occurred too rapidly to be accurately measured, due to rate-limiting diffusion of hydrogen. Compared to **4a**, $Ph_2P(CH_2)_2Rh(CO)(PPh_3)$ (**4b**) hydrogenated propene about 200 times faster at 45 °C; for 1-butene and *cis*-2-butene, the increase was also dramatic (**4a** does not hydrogenate either alkene). For $Me_2P(CH_2)_2Rh(CO)(PPh_3)$ (**5b**), the rate increase relative to **5a** for propene, 1-butene, and *cis*-2-butene is 100–200-fold. However, neither **4b** nor **5b** hydrogenated alkenes at rates significantly different from those of their Ta–Rh analogue **2b**.

In order to test whether isomerization could occur in the absence of H_2, each compound was heated with 1-butene in C_6D_6 in a sealed NMR tube. Isomerization to a mixture of 2-butenes occurred only with $Cp_2Ta(CH_2)_2Rh(CO)(PPh_3)$ (cis:trans = 1:1). No intermediate species were detectable by ^1H NMR spectroscopy.

Discussion

The proposed mechanism for the hydrogenation of alkenes by **1a** and **2a** is presented in Scheme VIII (shown for ethylene). We suggest that deuterium exchange lies on this catalytic cycle. This is supported by the following observations: (1) the rate of deuterium incorporation into the μ-CH_2 groups is much faster than hydrogenation; (2) the rate of hydrogenation is dependent upon the concentration of **1a**, H_2, and alkene; (3) the rate of alkene hydrogenation by **2a** is much greater (up to 150 times faster) than that by its ylide analogue **4a**. In contrast, although ylide complex **4a** shows the same rate constant for MeI oxidative addition,[21] it does not incorporate deuterium into its μ-CH_2 positions and it appears to require PPh_3 dissociation for hydrogenation. In addition, we presume that isomerization, because it follows the same rate law as hydrogenation, also lies on the cycle shown in Scheme VIII.

Scheme VIII

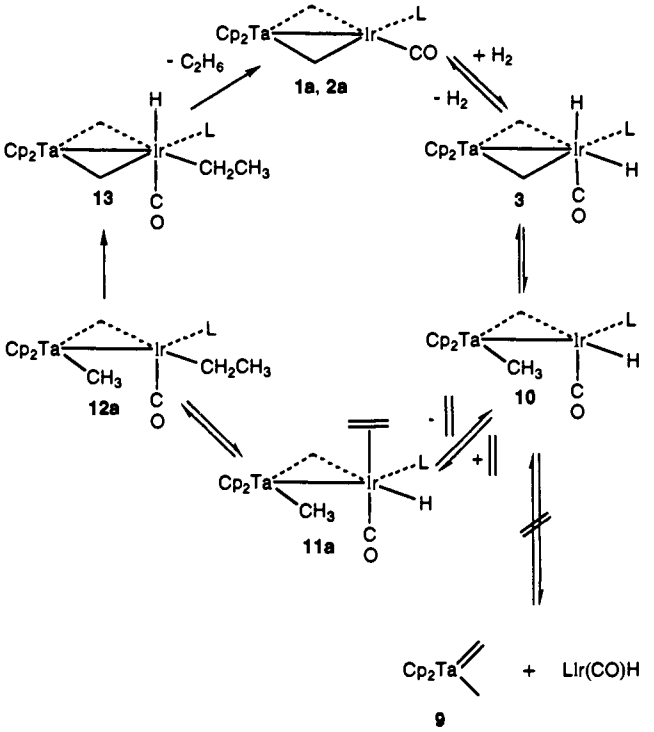

The first step in reactions of **1a** and **2a** is thought to be oxidative addition of hydrogen to the iridium center to form an octahedral Ir(III) *cis*-dihydride, typical of most square-planar Ir(I) compounds.[34-36] In the case of **1a**, the dihydride cannot be detected spectroscopically—the equilibrium constant at any achievable temperature is too small to be measured. However, the reaction of hydrogen with **2a** proceeds rapidly, as evidenced by the appearance in the NMR spectrum of resonances due to **3** (L = PPh_3) and by an immediate color change in solution from bright yellow to nearly colorless. This increase in reactivity likely stems from the increased electron density on the Ir center of **2a** caused by substituting a PPh_3 ligand for the strongly π-accepting CO.

The equilibrium constant for the H_2/**2a** system has been determined and found to decrease as the temperature was increased.[29] Under hydrogenation conditions at 45 °C, the ratio of **2a** to the Ir(III) *cis*-dihydride is approximately 1:3. The thermodynamic parameters for the reaction are within the expected range: the entropy is substantially negative and the enthalpy also negative. Using this $\Delta H°$ value of 12.0 ± 0.2 kcal/mol and the bond strength of the H–H bond (104.2 kcal/mol),[37] the average bond strength for the Ir–H bond can be calculated to be 58.1 ± 0.2 kcal/mol. This is essentially equal to the bond dissociation energy reported for the Ir–H bond in other $L_2Cl(CO)IrH_2$ compounds.[38] The upper limit for the bond strength of the average Ir–H bond in **1a** can be approximated as 50 kcal/mol, on the basis of a K_{eq} of 0.01 at 25 °C.

We believe that the next step in the cycle is the reductive elimination of a bridging methylene and an Ir–H bond to form a Ta–CH_3 group. The product of this reaction (**10**) is essentially

(34) Kubiak, C.; Woodcock, C.; Eisenberg, R. *Inorg. Chem.* **1980**, *19*, 2733.
(35) Crabtree, R. *Acc. Chem. Res.* **1979**, *12*, 331.
(36) Gargano, M.; Giannoccaro, P.; Rossi, M. *J. Organomet. Chem.* **1977**, *129*, 239.
(37) Lowry, T. H.; Richardson, K. S. *Mechanism and Theory in Organic Chemistry*, 3rd ed.; Harper & Row: New York, 1987; p 161.
(38) Yoneda, G.; Blake, D. M. *Inorg. Chem.* **1981**, *20*, 67 and references therein.

Scheme IX

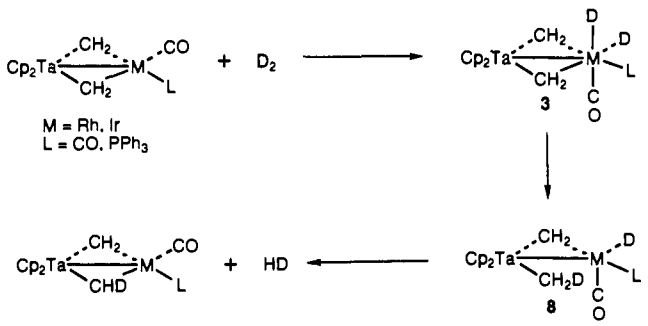

Scheme X

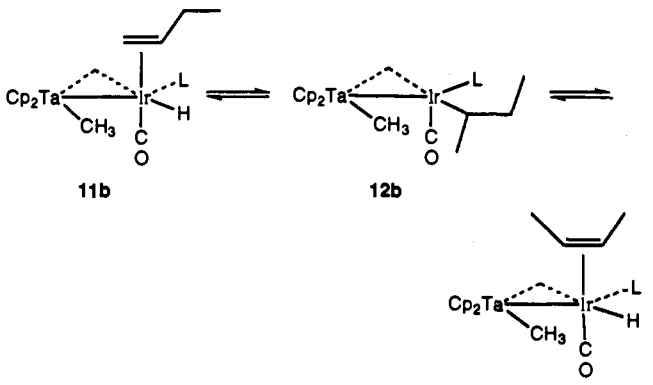

a complex between $Cp_2Ta(CH_2)(CH_3)$[39] and a Ir(CO)(L)H group. However, this intermediate does not break into the two mononuclear fragments since addition of $Cp_2Ta(CD_2)(CD_3)$ to a solution of **1a** under hydrogenation conditions does not result in either the appearance of CH_2 or CH_3 resonances (coming from free $Cp_2Ta(CH_2)(CH_3)$) or a decrease in the intensity of the μ-CH_2 groups of **1a** in the ^1H NMR spectra.

For the case of deuterium exchange, oxidative addition of the Ta–CH_2D across the Ir center, followed by reductive elimination of HD, results in the incorporation of one D into the molecule (Scheme IX). Under an excess of D_2, all four bridging methylene positions can become deuterated by this reversible process. In the cases of **2a** and **2b**, deuterium exchanges into each of the inequivalent bridge sites at approximately the same rate.

The formation of the Ta–Me group in **10** opens up two coordination sites at iridium. After the alkene binds to form **11a** (Scheme VIII), the next step is insertion of the alkene into the Ir–H bond to form the iridium alkyl **12a**. The alkyl group then can β-eliminate, re-forming the Ir–H bond and a bound alkene. This portion of the catalytic cycle is responsible for alkene isomerization (Scheme X). After oxidative addition of the Ta–Me group across the iridium center occurs to form **13**, the late metal becomes coordinatively saturated; further β-elimination from the iridium alkyl group is now unlikely. Formation of alkane by reductive elimination then occurs. This mechanism differs from that proposed for most mononuclear catalysts (Scheme I) in that (a) the first step involves oxidative addition of H_2, (b) the necessary open coordination site is not generated by ligand dissociation but by reductive elimination of two bound groups, and (c) reductive elimination of the alkane occurs from a 6-coordinate metal center. It is conceivable that H_2 could react with the intermediate **12a**, followed by the reductive elimination of ethane and the formation of **10**. Because the reaction is first order in H_2, this would require that the rate-determining step be ethylene binding or the insertion of ethylene into the iridium–hydride bond.

As expected, the activities of $Cp_2Ta(CH_2)_2Rh(CO)_2$ and $Cp_2Ta(CH_2)_2Rh(CO)(PPh_3)$ were much greater than those of their iridium analogues. However, the rate of deuterium incorporation into the μ-CH_2 groups of **2b** was slower than the rate of ethylene, propene, and 1-butene hydrogenation, suggesting that the mechanism for the rhodium system differs from that of the iridium system. Thus we suggest this catalyst follows a mechanism similar to that proposed for $RhCl(PPh_3)_3$. Unfortunately, PPh_3 inhibition studies were not possible due to competing side reactions (see Results). Alternatively, as suggested by a thoughtful reviewer, it is possible that the addition of H_2 to the rhodium analogue of **12a** in Scheme VIII could be much faster than the oxidative addition of the Ta–CH_3 group. As indicated for the Ir system, the reductive elimination of ethane would then regenerate **10**, and many cycles of hydrogenation could occur without exchange between methylene bridge hydrogens and Rh-bound hydrides.

Scheme XI

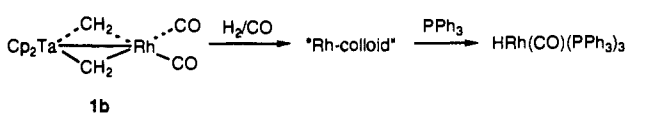

The study of Ta–Rh complex **1b** was complicated by the apparent formation of a colloid under hydrogenation conditions. This colloid or complexes derived from it were the active catalysts, as evidenced by the complete inhibition of ethylene hydrogenation in the presence of mercury (no reaction is seen between Hg and **1b** alone), which is proposed to poison heterogeneous catalysts by forming amalgams.[40] A large-scale (125 mg) preparation of this colloid in the presence of PPh_3 and excess CO produced the very active hydrogenation catalyst $HRh(CO)(PPh_3)_3$; no detectable tantalum complex could be recovered (Scheme XI).

In order to test the necessity of having an early metal as part of the structure of the catalysts, complexes were synthesized in which the Cp_2Ta fragment of **2a,b** is replaced with Ph_2P or Me_2P fragments, which have oxophilicity, Lewis acidity, chemical reactivity, and valence electron counts similar to those of Ta(V).[39,41,42] We find that the Ta and P complexes are electronically similar (ν(CO) (in C_6D_6) for **2a** and **4a** is 1934 cm^{-1}) and possess similar nucleophilicity (the second-order rate constant for the oxidative addition of MeI at −5 °C in THF to **2a** is 7.61 ± 0.43 M^{-1} s^{-1} and to **4a**, 7.55 ± 0.30 M^{-1} s^{-1}).[21] However, important differences between the two classes of compounds exist. X-ray crystallographic studies revealed that the four-membered rings are planar in the heterodinuclear compounds but nonplanar in the ylide complexes. In addition, unlike **2a**, compound **4a** exhibits solution fluxionality, with the PPh_3 ligand reversibly dissociating to form a 3-coordinate iridium center.[21]

Compounds **4a** and **5a** react, like their Ta analogue **2a**, with H_2 to establish an equilibrium between the *cis*-dihydride and the free compound. The kinetic product is the dihydride formed from oxidative addition of H_2 over the Ir–CO bond; this slowly isomerizes to the thermodynamic product in which H_2 has added over the Ir–P bond.[27,28] It is not obvious why both dihydride isomers are present with **4a,b**, whereas with **2a** only one dihydride isomer is seen.

Several lines of evidence indicate that alkene hydrogenation catalyzed by the ylide complexes follows a different mechanism from that of **1a**. First, the rate of alkene hydrogenation/isomerization by the Ph_2P–Ir complex **4a** (which, as described above, has similar nucleophilicity to **2a**) was markedly slower than that catalyzed by **2a**. Even the more electron-rich **5a** hydrogenated alkenes more slowly than **2a**. Second, the μ-CH_2 groups of the ylide complexes do not undergo deuterium exchange with D_2, indicating that the bridging methylene and Ir–H do not

(39) Schrock, R. R.; Sharp, P. R. *J. Am. Chem. Soc.* **1978**, *100*, 2389.

(40) Whitesides, G. M.; Hackett, M.; Brainard, R. L.; Lavalleye, J.-P. P. M.; Sowinski, A. F.; Izumi, A. N.; Moore, S. S.; Brown, D. W.; Staudt, E. M. *Organometallics* **1985**, *4*, 1819.

(41) Baldwin, J. E.; Swallow, J. C. *J. Org. Chem.* **1970**, *35*, 3583.

(42) Neithamer, D. R.; LaPointe, R. E.; Wheeler, R. A.; Richeson, D. S.; Van Duyne, G. D.; Wolczanski, P. T. *Organometallics* **1989**, *8*, 1192.

Scheme XII

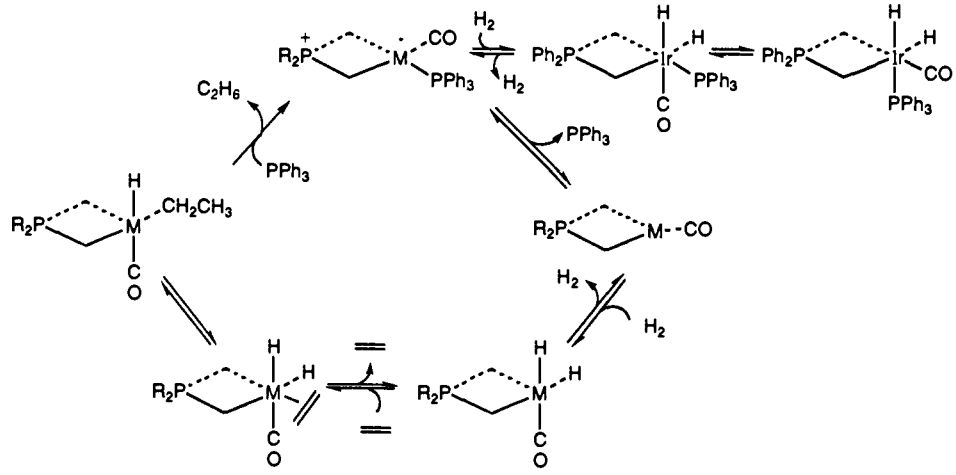

eliminate to form a P–CH_3 group. Finally, the rate of hydrogenation is inhibited by excess phosphine. For complexes **4a** and **5a**, the resting state of the catalyst is the dihydride but the rate of hydrogenation catalyzed by **4a** has been determined to be first order in hydrogen. Thus, in analogy to previous studies, the first step in the catalytic cycle is proposed to be dissociation of PPh_3 with the dihydride resting state existing as a nonproductive intermediate which does not lie on the catalytic cycle (Scheme XII).[14] Interestingly, the rate of hydrogenation catalyzed by the rhodium ylide complexes is similar to that promoted by Ta–Rh compound **2b**.

The main effect of having Cp_2Ta rather than R_2P attached to the late metal center appears to be the ability of the early metal to induce bridge reductive elimination. This may be the result of a M–M bond which stabilizes this transformation. We are not clear as to the physical basis for this stabilization, but a reviewer has made the interesting suggestion that the starting Ir(I) complex might have a dative (zwitterionic) M-to-Ta bond. Oxidative addition of H_2 weakens this interaction, and restoring it perhaps provides the driving force for reductive elimination of the bridge. As indicated in structural studies, such an interaction does not occur between phosphorus and the late metal in the ylide complexes, due probably to the relatively high energy of the appropriate acceptor orbital on phosphorus. The stabilization which prevents the fragmentation of **10** under hydrogenation conditions (Scheme VIII) might also be derived from a M–M interaction.

Conclusions

(1) The Ta–Ir complexes **1a** and **2a** hydrogenate alkenes by a pathway involving reductive elimination of one of the bridging methylenes. This route appears to be lower in energy than one involving CO or PPh_3 dissociation.

(2) The ylide P–Ir complexes **4a** and **5a** hydrogenate alkenes via a pathway that probably involves PPh_3 dissociation. The route that utilizes bridge elimination is energetically less favored and was not observed.

(3) The Ta–Rh complex **2b** and the ylide P–Rh complexes **4b** and **5b** hydrogenate alkenes via a pathway involving PPh_3 dissociation. Compound **2b** can eliminate its bridging methylene; however, we propose that the ligand dissociation pathway is lower in energy. As with the P–Ir complexes, neither ylide P–Rh complex can eliminate its μ-CH_2 groups.

(4) One of the complexes, **1b**, is unstable under hydrogenation conditions and forms an apparent colloid which can hydrogenate alkenes. Because the behavior of this system appears to be unique in this series, we are confident that the other complexes are well-behaved homogeneous catalysts.

(5) As expected, each rhodium compound is a significantly better hydrogenation catalyst than its iridium analogue.

(6) The presence of the early transition metal appears to be necessary for bridge elimination to occur. This may be the result of an M–M interaction which stabilizes this transformation.

(7) The Me_2P and Ph_2P fragments can model certain aspects (especially the ones which are manifestations of inductive interactions) of the Cp_2Ta fragment. This suggests that other non-metal fragments could also mimic transition metal moieties.

Experimental Section

General Procedures. Unless otherwise noted, all reactions and manipulations were performed in dry glassware under a nitrogen atmosphere in a Vacuum Atmospheres 553-2 drybox equipped with an M6-40-1H Dri-train or using standard Schlenk techniques. "Glass bombs" refer to cylindrical, medium-walled Pyrex vessels joined to Kontes K-826510 high-vacuum Teflon stopcocks.

All ^1H, ^2H, $^{13}C\{^1H\}$, and $^{31}P\{^1H\}$ NMR spectra were recorded on 300-, 400-, and 500-MHz instruments at the University of California, Berkeley, NMR facility. The 300-MHz instrument was constructed by Mr. Rudi Nunlist and interfaced with a Nicolet 1280 computer. The 400- and 500-MHz machines were commercial Bruker AM series spectrometers. All coupling constants are reported in hertz.

Benzene, toluene, pentane, and THF were distilled from sodium/benzophenone. Cyclohexene was distilled from CaH_2. Unless otherwise noted, all other reagents were used as received from commercial suppliers. The syntheses of **1a**, **1b**, and **2b** are described in separate papers.[21,22]

Reactions with gases (other than H_2 or D_2) or transferable liquids involved condensation of a calculated pressure (ideal gas law) of gas from a bulb of known volume into the reaction vessel at 77 K. Because H_2 and D_2 are gases at this temperature, these were added directly into the reaction vessel held at 77 K and, in the case of NMR tubes, flame-sealed 1 cm above the level of the liquid nitrogen. Sealed NMR tubes were prepared by connecting the tube to a Kontes vacuum adapter via a Cajon joint,[43] freezing and degassing the sample once (unless otherwise stated), and flame-sealing the tube with an oxygen/propane torch. Unless noted otherwise, all reactions were done at ambient temperature.

In order to make the Experimental Section more concise, certain sections contain only a general description of particular protocols and refer to tables in the supplementary material in which details for each experiment are listed.

$Cp_2Ta(CH_2)_2Ir(CO)(PPh_3)$ (2a). A solution of 200 mg (340 μmol) of $Cp_2Ta(CH_2)_2Ir(CO)_2$ (**1a**) in 25 mL of THF was placed in a 50-mL round-bottom flask equipped with a stir bar. To this was added a solution of 300 mg (1.14 mmol) of PPh_3 in 10 mL of THF. The reaction mixture was stirred for 48 h, during which the bright yellow solution became caramel orange. The solvent was removed in vacuo and the remaining solid washed with 3 × 30 mL of pentane to remove any excess PPh_3. Reddish-orange needles (190 mg, 68% yield) were obtained by crystallization from a saturated THF solution layered with ether and stored at −30 °C: mp 204–206 °C dec; ^1H NMR (C_6D_6) δ 7.54 (m, 6 H), 7.29 (m, 9 H), 5.42 (d, J_{PH} = 4.8, 2 H), 5.11 (s, 10 H), 4.34 (d, J_{PH} = 7.4,

(43) Bergman, R. G.; Buchanan, J. M.; McGhee, W. D.; Periana, R. A.; Seidler, P. F.; Trost, M. K.; Wenzel, T. T. In *Experimental Organometallic Chemistry: A Practicum in Synthesis and Characterization*; Wayda, A. L., Darensbourg, M. Y., Eds.; ACS Symposium Series 357; American Chemical Society: Washington, DC, 1987; p 227.

2 H); $^{13}C\{^1H\}$ NMR (C_6D_6) δ 195.5 (d, J = 6.7), 139.3 (d, J_{CP} = 46), 134.7 (d, J_{CP} = 12), 129.5 (s), 128.1 (d, J_{CP} = 9), 116.7 (d, J_{CP} = 5), 109.6 (d, J_{CP} = 32), 98.6 (s); $^{31}P\{^1H\}$ NMR (C_6D_6) δ 35.0 (s); IR (KBr) ν(CO) = 1937 cm^{-1}; IR (C_6D_6) ν(CO) = 1934 cm^{-1}; UV/vis (C_6H_6) 389 nm (ε = 2668 M^{-1} cm^{-1}), 428 (ε = 1549), 476 (ε = 554). Anal. Calcd for $C_{31}H_{29}IrOPTa$: C, 45.31; H, 3.56. Found: C, 45.14; H, 3.40.

$Cp_2Ta(CH_2)_2Ir(H)_2(CO)(PPh_3)$ (3). A solution of 15 mg (18 μmol) of **2a** in 0.48 mL of THF-d_8 was added to a PS-505 Wilmad NMR tube. To this was added 500 Torr of hydrogen at 77 K (182 μmol), and the tube was sealed. This amount of H_2 produced essentially complete conversion to the dihydride (which, however, reverts to H_2 and **2a** on attempted isolation): ^1H NMR (THF-d_8) δ 7.54 (m, 6 H), 7.31 (m, 9 H), 5.42 (dd, J = 8.4, 1.4, 1 H), 5.18 (s, 5 H), 5.07 (s, 5 H), 4.56 (m, 2 H), 4.48 (ddd, J = 8.4, 7.4, 2.4, 1 H), −8.84 (d, J = 14.6, 1 H), −15.0 (dm, J = 21.7, 1 H); $^{13}C\{^1H\}$ NMR (THF-d_8) δ 179.21 (s), 139.26 (d, J = 58), 134.72 (d, J = 11.1), 129.94 (s), 128.32 (d, J = 9.9), 101.02 (d, J = 2.3), 100.66 (s), 100.44 (s), 68.06 (d, J = 35.6); $^{31}P\{^1H\}$ NMR (THF-d_8) δ 20.7 (s).

$Cp_2Ta(CH_2)_2Ir(CO)_3$ (1a-$(CO)_3$). A solution of 22 mg (37 μmol) of **1a** in 0.44 mL of C_6D_6 was added to a PS-505 Wilmad NMR tube. Into this was transferred 510 Torr of CO from a 29.74-mL known-volume bulb (at 296 K), and the tube was sealed. Because the vapor pressure of CO at 77 K is 450 Torr, the pressure of CO in the tube at room temperature was approximately 1350 Torr. **1a**-$(CO)_3$ reverted to **1a** and CO upon attempted isolation. ^1H NMR (C_6D_6): δ 5.32 (br s, 4 H), 4.45 (s, 10 H). $^{13}C\{^1H\}$ NMR (C_6D_6): δ 190.6 (s), 107.3 (s), 98.7 (s).

$(C_6H_5)_2P(CH_2)_2Ir(CO)(PPh_3)$ (4a). A solution of 462 mg of $(C_6H_5)_2P(CH_2)_2Li$[23] (2.10 mmol) in 5 mL of THF was added dropwise to a stirred suspension of 1.63 g of $ClIr(CO)(PPh_3)_2$[44] (2.09 mmol) in 10 mL of THF. Within 20 min after the addition was completed, the cloudy yellow mixture was converted to an orange solution. The THF was removed under reduced pressure. The residue was added to 5 mL of benzene, and the mixture was filtered through Celite to remove the LiCl. Yellow crystals were isolated by vapor diffusion of 10 mL of pentane into the benzene solution at room temperature. A second crop of equal purity was obtained as a yellow powder by cooling the supernatant of the above solution to −40 °C. The overall yield was 1.31 g (90%): mp 185–194 °C dec; ^1H NMR (THF-d_8, 20 °C) δ 7.71 (m, 8 H), 7.47 (m, 10 H), 7.27 (m, 7 H), 1.49 (d, J = 7.2, 2 H), 0.37 (d, J = 8.3, 2 H); $^{13}C\{^1H\}$ NMR (THF-d_8, −75 °C) δ 187.6 (s), 139.3 (d, J = 56.1), 137.0 (d, J = 46.9), 134.7 (br), 130.9 (br), 130.1 (br), 128.6 (br), 123.1 (br) (resonances corresponding to the CH_2 groups were unresolvable at any achievable temperature); $^{31}P\{^1H\}$ NMR (THF-d_8, −90 °C) δ 33.3 (s), 29.6 (s); IR (C_6D_6) ν(CO) = 1934 cm^{-1}; UV/vis (C_6H_6) 367 nm (ε = 3984 M^{-1} cm^{-1}), 404 (ε = 3840), 458 (ε = 633). Anal. Calcd for $C_{33}H_{29}P_2OIr$: C, 56.96; H, 4.21. Found: C, 57.36; H, 4.12.

$(C_6H_5)_2P(CH_2)_2Rh(CO)(PPh_3)$ (4b). A solution of 278.2 mg of $(C_6H_5)_2P(CH_2)_2Li$[23] (1.26 mmol) in 5 mL of THF was added dropwise to a stirred suspension of 733 mg (1.06 mmol) of $ClRh(CO)(PPh_3)_2$[45] in 5 mL of THF. The yellow suspension became a deep red solution. The reaction mixture was stirred for 1 h, and the THF was removed in vacuo. The residue was slurried in 3 mL of benzene and the solution filtered through Celite to remove unreacted starting material and LiCl. Red crystals were obtained by vapor diffusion of 2 mL of pentane into the filtrate at room temperature. A second crop was obtained by cooling the remaining solution to −40 °C. The overall yield was 475 mg (74%): mp (combined crops) 182–190 °C; ^1H NMR (C_6D_6) δ 7.72 (m, 5 H), 7.55 (ddd, J = 11.4, 7.7, 1.4, 4 H), 7.15 (s, 2 H), 7.01 (m, 14 H), 1.11 (d, J = 5.5, 2 H), −0.10 (dd, J = 6.8, 0.87, 2 H); $^{13}C\{^1H\}$ NMR (THF-d_8, −75 °C) δ 195.9 (ddd, J = 67.6, 11.4, 2.7), 139.1 (d, J = 56.7), 137.6 (d, J = 37.2), 134.7 (d, J = 12.9), 131.9 (s), 131.1 (d, J = 10.6), 130.1 (s), 129.3 (d, J = 11.3), 128.8 (d, J = 8.7) (the CH_2 resonances were only observable via a DEPT −135, 25 °C), −0.27 (dd, J = 41.25, 12.49), −17.67 (m); $^{31}P\{^1H\}$ NMR (THF-d_8, −75 °C) δ 49.03 (d, J_{RhP} = 43.5), 34.84 (d, J_{RhP} = 21.9); IR (C_6D_6) ν(CO) = 1947 cm^{-1}; UV/vis (C_6H_6) 398 nm (ε = 4638 M^{-1} cm^{-1}); MS (EI) m/e 606 (M^+), 578 (M^+ − CO); HRMS (FAB) m/e calcd for $C_{33}H_{30}OP_2Rh$ 607.0827 (MH^+), found 607.0831.

$Me_2P(CH_2)_2Ir(CO)(PPh_3)$ (5a). A solution of 13.8 mg of $Me_2P(CH_2)_2Li$[23] (144 μmol) in 1.5 mL of THF was added dropwise to a stirred suspension of 98 mg of $ClIr(CO)(PPh_3)_2$ (125 μmol) in 2 mL of THF. The yellow suspension became a deep orange solution. The reaction mixture was stirred for 45 min, and the THF was removed in vacuo. The residue was slurried in 3 mL of benzene and the solution filtered through Celite to remove unreacted starting material and LiCl. Orange plates were obtained by vapor diffusion of 2 mL of pentane into the filtrate at −30 °C. The overall yield was 43 mg (60%): mp 165–170 °C; ^1H NMR (C_6D_6, 20 °C) δ 7.85 (ddd, J = 10.3, 8.3, 1.3, 6 H), 7.11 (m, 6 H), 7.02 (m, 3 H), 1.20 (d, J = 7.1, 2 H), 0.77 (d, J = 12.0, 6 H), −0.84 (d, J = 7.4, 2 H); $^{13}C\{^1H\}$ NMR (C_6D_6, 20 °C) δ 187.44 (s), 137.44 (d, J = 44.3), 134.45 (d, J = 11.9), 129.26 (d, J = 1.9), 127.96 (d, J = 7.2), 24.33 (d, J = 33.5), −5.00 (d, J = 41.6), −16.73 (d, J = 44.6); $^{31}P\{^1H\}$ NMR (toluene-d_8, 20 °C) δ 29.3 (br), 22.5 (s); $^{31}P\{^1H\}$ NMR (toluene-d_8, −90 °C) δ 30.5 (s), 25.5 (s); IR (C_6D_6) ν(CO) = 1929 cm^{-1}; UV/vis (C_6H_6) 303 nm (ε = 5100 M^{-1} cm^{-1}), 360 (ε = 3390), 402 (3120), 456 (617); MS (EI) m/e 572 ($M + H^+$); HRMS (EI) m/e calcd for $C_{23}H_{25}IrOP_2$ 570.0987 (^{191}Ir), found 570.0997.

$Me_2P(CH_2)_2Rh(CO)(PPh_3)$ (5b). A solution of 22.0 mg of $Me_2P(CH_2)_2Li$[23] (229 μmol) in 7 mL of THF was added dropwise to a stirred suspension of 147 mg of $ClRh(CO)(PPh_3)_2$ (213 μmol) in 3 mL of THF. The yellow suspension became a deep yellow solution. The reaction mixture was stirred for 3 h, and the THF was removed in vacuo. The residue was slurried in 2.5 mL of toluene and the solution filtered through Celite to remove unreacted starting material and LiCl. Orange plates were obtained by slow vapor diffusion of hexane into the filtrate at −30 °C. The overall yield was 68.5 mg (67%): mp 141–144 °C; ^1H NMR (C_6D_6) δ 7.81 (vt, J = 8.2, 6 H), 7.07 (m, 9 H), 0.93 (d, J = 11.9, 6 H), 0.49 (d, J = 5.4, 2 H), −0.73 (d, J = 6.5, 2 H); $^{13}C\{^1H\}$ NMR (C_6D_6) δ 196.0 (dd, J = 67.4, 1.3), 138.6 (d, J = 34.6), 134.8 (d, J = 13.2), 129.6 (d, J = 1.4), 128.5 (d, J = 9.0), 24.2 (dd, J = 34.3, 2.4), −8.86 (dd, J = 44.0, 14.4), −16.4 (J = 46.5, 15.2); $^{31}P\{^1H\}$ NMR (C_6D_6, 25 °C) δ 41.8 (br), 19.3 (d, J = 23.4); IR (C_6D_6) ν(CO) = 1942 cm^{-1}; UV/vis (C_6H_6) 395 nm (ε = 3524 M^{-1} cm^{-1}); MS (EI) m/e 482 (M^+), 454 (M^+ − CO): HRMS (EI) m/e calcd for $C_{23}H_{25}OP_2Rh$ 482.0436, found 482.0432. Anal. Calcd for $C_{23}H_{25}OP_2Rh$: C, 57.27; H, 5.24. Found: C, 57.07; H, 5.18.

$(C_6H_5)_2P(CH_2)_2Ir(H)_2(CO)(PPh_3)$ (6a,b). A solution of 11.8 mg of **4a** (17.0 μmol) in 0.49 mL of C_6D_6 was transferred into a PS-505 Wilmad NMR tube. To this was added 500 Torr of hydrogen at 77 K (V = 2.23 mL; 255.3 μmol of H_2). The tube was sealed and warmed to room temperature. Analysis by ^1H NMR spectroscopy indicated that the equilibrium ratio of **6a**:**6b** at room temperature was 2:1. All attempts to isolate either **6a** or **6b** resulted in reversion to H_2 and **4a**. **6a**: ^1H NMR (C_6D_6) δ 7.75 (m, 6 H), 7.41 (ddd, J = 11.3, 8.4, 1.5, 2 H), 7.26 (m, 2 H), 7.00 (m, 15 H), 1.87 (m, 1 H), 1.49 (m, 1 H), 1.06 (m, 1 H), 0.59 (vt, J = 11.2, 1 H), −7.71 (d, J_{HP} = 20.5, 1 H), −12.8 (d, J_{HP} = 14.3, 1 H); $^{31}P\{^1H\}$ NMR (C_6D_6) δ 43.30 (d, J_{PP} = 9.4), 16.98 (d, J_{PP} = 9.4). **6b**: ^1H NMR (C_6D_6) δ 7.83 (ddd, J = 9.7, 8.5, 1.5, 6 H), 6.96 (m, 15 H), 6.82 (ddd, J = 7.9, 7.9, 1.7, 2 H), 6.74 (m, 2 H), 1.34 (m, 1 H), 1.23 (m, 1 H), 0.35 (m, 1 H), 0.20 (m, 1 H), −8.16 (d, J_{HP} = 154.9, 1 H), −11.6 (d, J_{HP} = 14.3, 1 H); $^{31}P\{^1H\}$ NMR (C_6D_6) δ 43.51 (d, J_{PP} = 12.4), 11.13 (d, J_{PP} = 12.4).

$(CH_3)_2P(CH_2)_2Ir(H)_2(CO)(PPh_3)$ (7a,b). A solution of 10.1 mg (17.7 μmol) of **5a** in 0.45 mL of C_6D_6 was transferred to a PS-505 Wilmad NMR tube. Added to this was 510.4 Torr of H_2 at 77 K (V = 1.28 mL; 136.0 μmol of H_2). The tube was sealed and warmed to room temperature. After 1 day, the ratio of **7a**:**7b** was 2:1. **7a**: ^1H NMR (C_6D_6) δ 7.82 (dd, J = 10.5, 7.7, 6 H), 7.08 (m, 6 H), 6.99 (m, 3 H), 1.14 (m, 1 H), 0.89 (d, J_{HP} = 12.0, 3 H), 0.76 (m, 1 H), 0.43 (d, J_{HP} = 11.3, 3 H), 0.38 (m, 1 H), −0.16 (m, 1 H), −7.8 (ddd, J = 20.7, 3.0, 3.0, 1 H), −12.6 (d, J_{HP} = 14.6, 1 H); $^{31}P\{^1H\}$ NMR (C_6D_6) δ 42.13 (d, J_{PP} = 11.4), 16.53 (d, J_{PP} = 11.4). **7b**: ^1H NMR (C_6D_6) δ 1.26 (d, J_{HP} = 12.3, 3 H), 1.23 (m, 1 H), 0.58 (m, 1 H), −0.11 (d, J_{HP} = 11.2, 3 H), −0.34 (m, 1 H), −0.49 (m, 1 H), −8.4 (d, J_{HP} = 155.3, 1 H), −12.6 (d, J_{HP} = 14.6, 1 H); $^{31}P\{^1H\}$ NMR (C_6D_6) δ 39.95 (d, J_{PP} = 10.0), 11.81 (d, J_{PP} = 10.0). The proton resonances for the aryl hydrogens of **7b** overlapped with those of **7a**.

Reaction of 1a with D_2. A solution of 40 mg of **1a** (68 μmol) in 10 mL of ether was added to a 50-mL glass bomb. The solution was frozen to 77 K and degassed. Deuterium gas was added to the frozen solution (5.83 mmol). The stopcock was closed and the solution heated at 45 °C for 24 h. The solution was once more frozen and degassed, and another 5.83 mmol of D_2 was added. The solution was heated at 45 °C for 24 h, after which the excess gas and solvent were removed in vacuo to give **1a**-d_4 deuterated >99% in the methylene position: ^2H NMR (C_6H_6) δ 5.42; MS (EI) 592 (M^+), extent of deuteration >99%.

Small-Scale Reactions with D_2. A solution of each complex was added to a Wilmad PS-505 NMR tube. An excess of deuterium gas was added to the frozen solution, and the tube was sealed. The solution was thawed and then heated at 45 °C until the reaction went to completion (or for 1 month if no reaction occurred). The reaction was monitored by ^1H NMR spectroscopy. See supplementary Table S-1 for details.

(44) Collman, J. P.; Sears, C. T., Jr.; Kubota, M. *Inorg. Synth.* **1968**, *11*, 101.

(45) Evans, D.; Osborn, J. A.; Wilkinson, G. *Inorg. Synth.* **1968**, *11*, 99.

Reaction of 4a with C_2H_4. A solution of 41.5 mg of **4a** (59.6 μmol) in 0.4 mL of THF-d_8 was transferred to an NMR tube. Into this was condensed 895 μmol of ethylene, and the tube was sealed. No reaction was observed at room temperature; cooling the solution to −75 °C resulted in the formation of **8** (which reverts to ethylene and **4a** upon attempted isolation). The ^1H NMR spectrum was too complex for proper analysis; however, the $^{13}C\{^1H\}$ NMR spectrum clearly indicates adduct formation. $^{13}C\{^1H\}$ NMR (THF-d_8, −75 °C): δ 185.9 (d, J = 8.2), 145.1 (d, J = 32.3), 136.8 (d, J = 38.1), 135.0 (m), 134.3 (m), 131.9 (m), 129.6 (m), 128.6 (m), 128.0 (m), 23.8 (s), 13.0 (s), −36.3 (dd, J = 51.9, 75.8), −52.6 (d, J = 51.9).

Reaction of 2b with CO. A solution of 3.6 mg (4.9 μmol) of **2b** in 0.45 mL of C_6D_6 was added to a PS-505 Wilmad NMR tube. Into this was transferred CO (from a 29.74-mL known-volume bulb, 525 Torr at 296 K). Because the vapor pressure of CO at 77 K is 450 Torr, the pressure of CO in the tube at room temperature was approximately 1.8 atm. ^1H NMR (C_6D_6): δ 7.80 (br s, 6 H), 7.03 (m, 9 H), 5.56 (s, 4 H), 4.46 (s, 10 H). $^{31}P\{^1H\}$ NMR (C_6D_6): δ −4.1 (br s). These spectroscopic data indicate the formation of **1b**, which undergoes ligand exchange with liberated PPh_3.

Reaction of 1b with H_2, CO, Propene, and PPh_3. In the drybox, 333 mg (1.27 mmol) of PPh_3 was added to a 157-mL glass bomb equipped with a stir bar, followed by addition of a 25-mL benzene solution of **1b** (125 mg, 0.25 mmol). On a vacuum line, the flask was frozen (77 K) and degassed two times. To this frozen solution was added 5.03 mmol of propene followed by 500 Torr of synthesis gas (H_2:CO = 3:1; 12.2 mmol of H_2, 4.08 mmol of CO) at 77 K. The flask was heated to 68 °C in an oil bath for 3.5 days. The stirred solution turned from orange-brown to dark orange-red within 1 day. Removal of the volatiles under vacuum afforded a dark orange-red oil. A yellow-orange powder was obtained after repeated washings with pentane (20 mL total). This powder was recrystallized from ether (10 mL) at −30 °C to yield a yellow-orange solid identified as $HRh(CO)(PPh_3)_3$ (25% yield) on the basis of ^1H and $^{31}P\{^1H\}$ NMR and IR comparisons with an authentic sample.

Reactions with 1-Butene (Isomerization in the Absence of H_2). A solution of each complex in C_6D_6 was added to an NMR tube. Each solution was frozen and degassed. The alkene was condensed into the NMR tube, after which the tube was sealed. The solution was heated to 45 °C and was monitored by ^1H NMR spectroscopy for signals due to *cis*- or *trans*-2-butene. See supplementary Table S-2 for details.

$(CD_3)_2Zn$.[46] Into a 1-L glass bomb were placed 8.00 g of Zn powder (122 mmol) and 2.00 g of Cu 150 mesh powder (31.0 mmol). The stopcock was closed and the bomb brought out of the drybox. The bomb was frozen and degassed. Into this mixture was vacuum-transferred 5.0 mL of CD_3I (78.6 mmol). Upon thawing, the bomb was wrapped in several layers of electrical tape (to help prevent an explosion due to a high buildup of pressure). This container was then heated to 120 °C in an oil bath for 16 h. Pure $(CD_3)_2Zn$ (2.7 mL, 95%) was vacuum-transferred from this bomb to a graduated bomb cooled to 77 K. Heating the remaining Zn/Cu couple with a heat-gun is necessary to remove all of the $(CD_3)_2Zn$. (*Danger*! $(CD_3)_2Zn$ reacts violently with air.)

$Cp_2Ta(CD_2)(CD_3)$. This compound was synthesized analogously to $Cp_2Ta(CH_2)(CH_3)$[39] using the $(CD_3)_2Zn$ synthesized above. The ^1H NMR spectrum revealed that the extent of deuteration was >95%: MS (EI) 345 (M^+).

Kinetic Studies

General Procedures. All kinetics experiments were carried out by monitoring the ^1H NMR spectrum on either a 300-MHz Nicolet or an AM-400 Bruker instrument. Standard solutions were prepared in the drybox in volumetric flasks and stored in the drybox freezer at −30 °C. Individual runs were prepared in the drybox by transferring aliquots of standard solutions using a graduated pipet into a PS-505 NMR tube. The remaining gases or liquids were then vacuum-transferred into the NMR tube above the frozen and degassed solution. The NMR tube was sealed and kept at 77 K until immediately before the kinetic run (at which point the solutions were thoroughly shaken by hand for at least 1 min). For deuterium exchange reactions, the loss or growth of the CH_2 resonance was calibrated with ferrocene as the internal standard. Hydrogenation and isomerization reactions were monitored by following the loss of the alkene resonance or appearance of the alkane resonance and calibrated with either ferrocene, toluene, or residual benzene as the internal standard.

Plots of c/c_0 or $\ln c/c_0$ (c = measured concentration at time t, c_0 = initial concentration) vs time were plotted using the Cricket graph or Igor program.[47,48] Least-squares fits of the data were also performed by the software in the program to give as the slope the pseudo-first-order rate constant. Second-order rate constants were calculated by standard kinetic equations.[49]

Determination of the Rate Law for Deuterium Incorporation into 1a. A standard solution of **1a** in toluene-d_8 was placed in a Wilmad PS-505 NMR tube. The solutions were frozen and degassed twice. Deuterium gas was then added to each solution at 77 K. Solutions were kept at 77 K until needed. Reactions were monitored by following the loss of the μ-CH_2 resonance vs ferrocene as the internal standard. The concentration of D_2 was determined from measurements for H_2 under the same conditions. See Table I for details.

Determination of the Rate Law for Hydrogenation of Ethylene by 1a. A measured amount of a standard solution of **1a** in C_6D_6 was placed in an NMR tube. After the ethylene was condensed into the frozen and degassed solution, H_2 was added. The samples were kept at 45 °C in a constant-temperature Endocal RTE 8DD water bath. See Table II for details.

Hydrogenation/Isomerization Reactions: Turnover Measurements. A measured amount of a standard solution of the catalyst containing an internal standard was added to a Wilmad PS-505 NMR tube. The sample was frozen and degassed twice. To this were added calculated amounts of alkene and H_2. The solution was kept frozen until the initial spectrum was taken, and subsequently, the tube was placed in a constant-temperature bath. The reactions were monitored by ^1H NMR spectroscopy and calibrated against an internal standard. The turnover rates were calculated after 10 ± 5% of the total reaction had occurred. See supplementary Table S-3 for details.

Hydrogenation/Isomerization Reactions: PPh_3 Inhibition. A procedure identical to that used in the turnover measurement study was employed, with the exception that a weighed amount of PPh_3 (usually 10–15 equiv) was added to the catalyst solution in the drybox. Only the ylide catalysts were used for this experiment because the Ta–Rh compounds decomposed in the presence of excess PPh_3. The Ta–Ir dicarbonyl **1a** reacted with PPh_3 to form compound **2a**, and **2a** in the presence of PPh_3 formed solution species consistent with a 5-coordinate complex. See supplementary Table S-4 for details.

Acknowledgment. We thank Johnson-Matthey-Aesar/Alfa for a generous loan of rhodium and iridium and the National Science Foundation (Grant No. CHE-8722801) for partial financial support of this work. We are also grateful for an exceptionally thorough reading of our initial manuscript by two thoughtful reviewers. This provided important mechanistic suggestions, as well as the detection and correction of a number of ambiguities and typographical and transcription errors.

Supplementary Material Available: Tables containing details on the experimental setups used for the turnover studies, the reactions of the catalysts with D_2 and 1-butene, the PPh_3 inhibition studies, and the mercury spoiling tests (3 pages). These are provided with the archival edition of the journal, which is available in many libraries. Alternatively, ordering information is given on any current masthead page.

(46) This compound was first prepared in our laboratories by K. I. Goldberg.

(47) The Igor graphing program was modified by Dr. Kevin Kyle to calculate the infinity point and rate constant for a first-order reaction.

(48) The Igor graphing and data analysis software is distributed by Wavemetrics, Lake Oswego, OR.

(49) Benson, S. W. *The Foundations of Chemical Kinetics*; McGraw-Hill: New York, 1960.